Synthesis and characterization of ferrisilicate analogs of ferrierite (Fe-FER) zeolites

Siddhesh Shevade, Ranjeet Kaur Ahedi and A.N. Kotasthane*

Catalysis Division, National Chemical Laboratory, Pune 411 008, India
E-mail: cata@ems.ncl.res.in

Received 1 July 1997; accepted 2 October 1997

Ferrisilicate analogs of ferrierite (FER) type zeolite having SiO_2/Fe_2O_3 ratios ranging between 30 and 200 have been synthesized using pyrrolidine as the templating agent. On calcination, the samples develop a typical buff color indicating conversion of some tetrahedral Fe^{3+} into octahedral Fe^{3+}. Correspondingly, a doublet in the Mössbauer spectrum with isomer shift at 0.15 and 0.68 mm s^{-1} was observed. The Fe-FER samples were further characterized by UV-vis, IR and TG/DTA. Fe-FER samples were found to exhibit catalytic activity for *n*-hexane oxidation reactions with hydrogen peroxide as oxidizing agent.

Keywords: Fe-FER crystallization, ESR, IR, UV-vis

1. Introduction

The ferrisilicate analogs of zeolites and molecular sieves are well documented [1–12]. Ferrierite is a medium pore zeolite based on chains of 5-rings, which are linked to give [5^4] polyhedral units. There are two types of intersecting channels in the structure. The main channels parallel to the orthorhombic *c*-axis of the crystal are outlined by elliptical 10-MR pores (4.3 × 5.5 Å) while the side channels parallel to the *b*-axis are formed by 8-MR pores (3.4 × 4.8 Å). Ferrierite has been found to be an excellent catalyst for skeletal isomerization of *n*-alkenes to iso-alkenes [14,15]. The high acidity of aluminosilicates leads to lower catalytic selectivity, which further decreases with time on stream. Therefore these compounds cannot be used in reactions which require moderate acidity. Substitution for Al^{3+} by trivalent cations like Fe^{3+}, Ga^{3+}, Cr^{3+}, etc. is known to impart moderate acidity in zeolites [16]. Ferrierite can be synthesized using a number of templates like hexamethylene diamine [17], trimethyl cetyl ammonium hydroxide [18], trimethyl amine hydrochloride [19], ethylenediamine [20], cyclohexylamine [21] etc. Ga^{3+} has been successfully incorporated in ferrierite (FER) zeolite [22] and Fe–Al ferrierite has also been reported [23]. Recently, Borade and Clearfield [24] have reported the synthesis of iron ferrierite using hexamethyleneimine as a structure directing agent. However, this procedure requires longer crystallization periods yielding lower SiO_2/Fe_2O_3 ratios.

In this paper, we describe the hydrothermal synthesis of Fe-FER using pyrrolidine as templating agent with shorter crystallization periods and higher SiO_2/Fe_2O_3 ratios. Fe-FER characterization and catalytic properties have also been discussed.

* To whom correspondence should be addressed.

2. Experimental

The synthesis of Fe-FER was conducted following two systems. The first, the Fe-FER-I system, involved addition of $Al_2(SO_4)_3 \cdot 16H_2O$ (Loba Chemie) in different concentrations, whereas for the Fe-FER-II system 0.5 wt% of seed precursors of H-Al-FER have been used.

Fe-FER-I series. Typical synthesis included addition of a solution, prepared by mixing 1.32 g of $Al_2(SO_4)_3 \cdot 16H_2O$ in 15 g of distilled water, 1.02 g of ferric sulphate (Loba Chemie) dissolved in 10 g of distilled water and 1.8 g of concentrated H_2SO_4 (98% S.D. fine chemicals) in 10 g of distilled water to 52.5 g of Na_2SiO_3 (28% SiO_2, 9% Na_2O) in 25 g of distilled water. The bluish gel formed was stirred for approximately 1 h. The gel was transferred to an 300 ml stainless steel autoclave (Parr 4861 300 ml) and heated at 433 K for 40 h. The autoclave was quenched with cold water, the material filtered, washed and dried at 373 K. Utmost care was taken to clean the autoclave to avoid any seeding effect from the previous batches. The samples with SiO_2/Fe_2O_3 ratios ranging from 80 to 240 were synthesized and designated as Fe-FER-I (a–d, table 1) series. The initial gel composition was: (15.8–95)Na_2O:(31.6–285)py:(0.316–3.0)Al_2O_3:Fe_2O_3:(80–240)SiO_2:(633–9494) H_2O, where py = pyrrolidine.

Fe-FER-II series. In this procedure seeds of a highly crystalline Al-FER were used instead of Al-source. In a typical synthesis 2.06 g of ferric sulphate (Loba Chemie) dissolved in 10 g of distilled water along with 1.8 g of

Table 1
Physico-chemical properties of the Fe-FER series

Sample [a]	Gel		Zeolite		K/Fe molar ratio	% cryst.
	SiO_2/M_2O_3 [b]	SiO_2/Fe_2O_3	SiO_2/M_2O_3	SiO_2/Fe_2O_3		
Fe-FER-Ia	60	80	32	42	0.65	90
Fe-FER-Ib	60	120	34	63	0.68	95
Fe-FER-Ic	60	240	30	124	0.70	89
Fe-FER-Id	no added Al	60	no added Al	32	n.d.	75 + ZSM-5
Fe-FER-IIa	no added Al	40	no added Al	25	0.81	85
Fe-FER-IIb	"	60	"	34	0.86	95
Fe-FER-IIc	"	90	"	42	0.80	92
Fe-FER-IId	"	150	"	73	0.78	90

[a] Note: Fe-FER-I series without seeds and Fe-FER-II series are with seeds.
[b] $M_2O_3 = Al_2O_3 + Fe_2O_3$.

concentrated H_2SO_4 (98% S.D. fine chemicals) in 10 g of distilled water was added to 52.5 g of Na_2SiO_3 (28% SiO_2, 9% Na_2O) in 25 g of distilled water. The bluish gel formed was stirred for approximately 1 h. To this gel 10 ml of pyrrolidine (99%, SRL) was added followed by addition of the remaining 45 g of distilled water. The gel was stirred for 1 h and finally 0.5 g of highly crystalline H/Al-FER ($SiO_2/Al_2O_3 = 34$) were added as seeds. The remaining procedure was the same as in the first method. Fe-FER samples of input gel ratios changing from 30 to 200 were synthesized by the above procedure and the samples were designated as Fe-FER-II (a–d, table 1) series. The gel composition for the second method was in the range: (5.9–79)Na_2O:(11.9–238)py:Fe_2O_3:(30–200)SiO_2:(237–7920)H_2O, where py = pyrrolidine.

As-synthesized Fe-FER-I and II samples were off-white. In order to obtain the Fe-FER series in Na-form the samples were subjected to calcination at 753 K for 10–12 h and then converted into their NH_4^+ forms by multiple exchanges with 2 N ammonium nitrate at 363 K. The NH_4^+ forms were dried at 383 K and then calcined in step-wise mode at 753 K to obtain the H^+ active forms. The active H^+/Fe-FER powder was found to develop a slight buff color.

Fe-impregnation. The Fe-impregnated catalyst involving non-framework iron ions was made using amorphous aluminosilicate (Si/Al = 15) powder. The amorphous powder was impregnated with required aqueous ferric-salt solution ($Fe_2(SO_4)_3 \cdot 5H_2O$) dried and then calcined at 773 K for 12 h to give about 3.0–4.0 wt% Fe_2O_3 in the final catalyst.

3. Characterization

The solid Fe-FER obtained was characterized by X-ray powder diffraction (Rigaku D Max III VC) using Cu Kα radiation. The chemical composition for silicon and iron was established by using a wavelength dispersive XRF (3070 Rigaku) spectrometer. Thermogravimetric analysis (TGA) and differential thermal analysis (DTA) were carried out in flowing air (3 dm^3 h^{-1}) at a heating rate of 10 K min^{-1} on automatic TG/DTA (SETRAM 92). The crystal size and morphology were examined by a scanning electron microscope 440 Stereoscan (Cambridge UK). The material was further characterized by UV-vis (Shimadzu UV2101PC spectrophotometer). FTIR (Nicolet FTIR), Mössbauer (Mössbauer spectrometer, Austin Sci. Inc., USA, Mössbauer system S-600) and ESR (Bruker electron spin resonance ER 200D-SRC) spectroscopies. The ion-exchange measurements were performed by titrating the H-forms of both the series (1.0 g) in 10 ml distilled water with 0.05 N KOH upto pH 8.0 and then stirring the mixture for 1.0 h, washing thoroughly and drying to obtain the K-form of Fe-FER. Both the K–Fe-FER zeolites were analysed by AAS (Hitachi 8000 Japan).

4. Catalysis

The catalytic reaction was carried out in a two-necked flask fitted with a water condensor under magnetically stirred conditions and the products were analysed by a HP 5880 gas chromatograph using a 50 m methyl silicon gum capillary column.

5. Results and discussion

Samples of the Fe-FER system were prepared by two methods. The samples prepared by the first method i.e. Fe-FER-I (a–d) series were synthesized by partly substituting Fe^{3+} for Al^{3+}. Pure crystalline Fe-FER could be obtained for SiO_2/M_2O_3 (M = Fe + Al) ratio of 60 and SiO_2/Fe_2O_3 ratio between 80 and 240. It was observed that as the concentration of Fe^{3+} in the starting gel was increased and that of Al^{3+} was decreased, the metastability for ferrierite phase decreases and ZSM-5 appears as an impurity phase (table 1). In the case of the

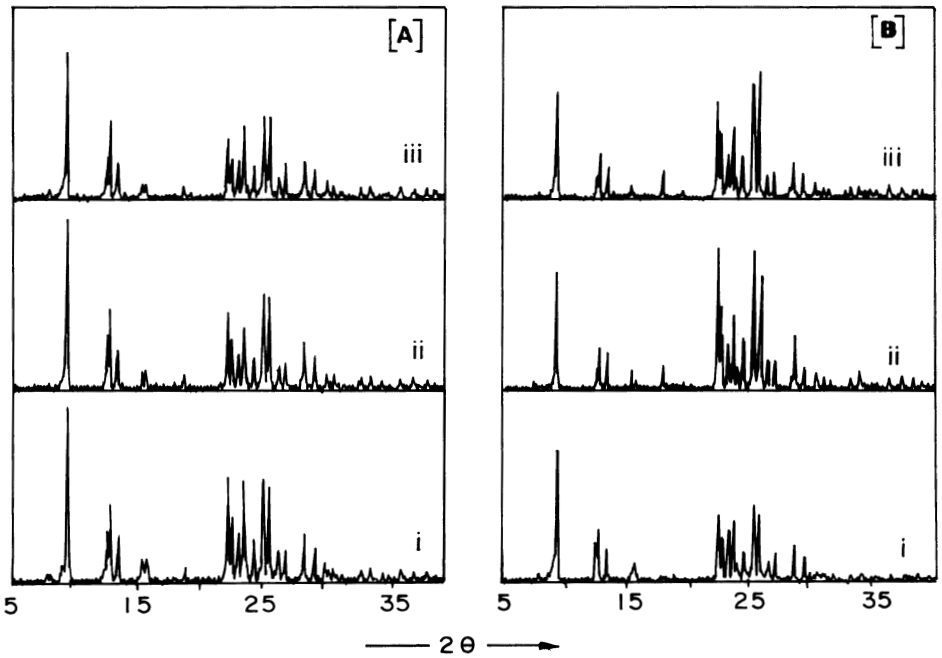

Figure 1. X-ray diffraction patterns for (A) calcined and (B) as-synthesized samples; (i) Al-FER; (ii) Fe-FER-Ib (table 1) and (iii) Fe-FER-IIb (table 1).

second method in absence of added aluminum, a small quantity (0.5 g) of highly crystalline H–Al-FER ($SiO_2/Al_2O_3 = 60$) was added as seeds and pure Fe-FER could be crystallized in the SiO_2/Fe_2O_3 range of 30 to 200. These samples were designated as Fe-FER-II (a–d). Figure 1 shows the X-ray diffraction patterns for both calcined and as-synthesized (i) Al-FER, (ii) Fe-FER-I and (iii) Fe-FER-II, which are found to be in good agreement with those reported for the FER phase. It was observed that total replacement of Al^{3+} by Fe^{3+} could not be achieved in the absence of seeds and led to the formation of ZSM-5, indicating that some optimum quantity of Al^{3+} ions are necessary to stabilize the ferrierite type topology. On calcination the intensity of low angle peaks in the XRD patterns (in case of all the samples) was found to increase, which may be due to the removal of organic moieties from the voids of the FER and the samples were found to develop a slight buff color. The other changes observed can be due to a minor variation in the lattice constants. The lattice parameters were verified using least-squares fitting. Least-squares analysis data and the computed values of the unit cell volume from the XRD data (table 2) reveal expansion of the unit cell of the Fe-FER-I and II series indicating successful insertion of Fe-ions during hydrothermal synthesis. The ion-exchange capacities for the Fe-FER-I and Fe-FER-II series are summarized in table 1. It is observed that the ion-exchange capacities of the Fe-FER-I series were lower as compared with Fe-FER-II indicating the presence of a higher number of exchangeable sites for the II series. It is known from the literature [25] that a K/Fe molar ratio near unity indicates tetrahedral location capable for ion exchange in ferrisilicates. Considering this, Fe-FER-I indicates nearly 25% loss of ion exchange sites of calcination (table 1). However, values closer to unity for Fe-FER-II attest that the larger portion of substituted Fe can be located in sites capable for ion exchange.

The Mössbauer spectra at room temperature of both as-synthesized as well as calcined samples (Fe-FER-IIc, table 1) are shown in figure 2 (a and b). The spectrum of as-synthesized Fe-FER with $SiO_2/Fe_2O_3 = 42$ (Fe-FER-IIb) shows a broad singlet with isomer shift of 0.25 mm s^{-1} (curve a) which is in agreement with the estimate made by Meagher et al. [26]. An isomer shift of ca. 0.25 mm s^{-1} has been assigned for Fe^{3+} ions in tetrahedral position. On calcination at 753 K the signal splits into an inequivalent doublet with components at 0.15 and 0.68 mm s^{-1} (the average isomer shift is 0.41 mm s^{-1}), which corresponds to a combination of tetrahedrally as well as octahedrally coordinated Fe^{3+} as discussed by Garten et al. [27] (curve b). These results indicate complete initial incorporation of Fe^{3+} in the framework during hydrothermal synthesis. The data from

Table 2
Data on unit cell parameters for Fe-FER series

Sample	Unit cell parameters (Å)			Unit cell volume (Å^3)
	a_0	b_0	c_0	
Al-FER	18.82	14.06	7.43	1957
Fe-FER-Ib	18.88	14.10	7.44	1980
Fe-FER-IIb	18.97	14.13	7.45	1997

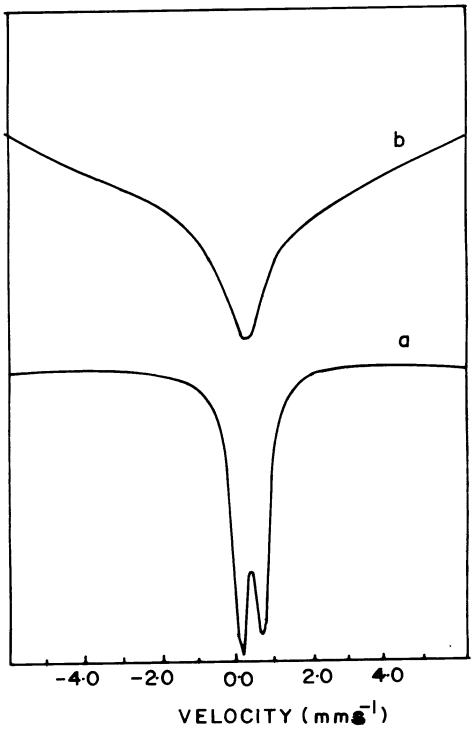

Figure 2. Room temperature Mössbauer spectra for the Fe-FER-IIc sample; (a) as-synthesized and (b) calcined samples.

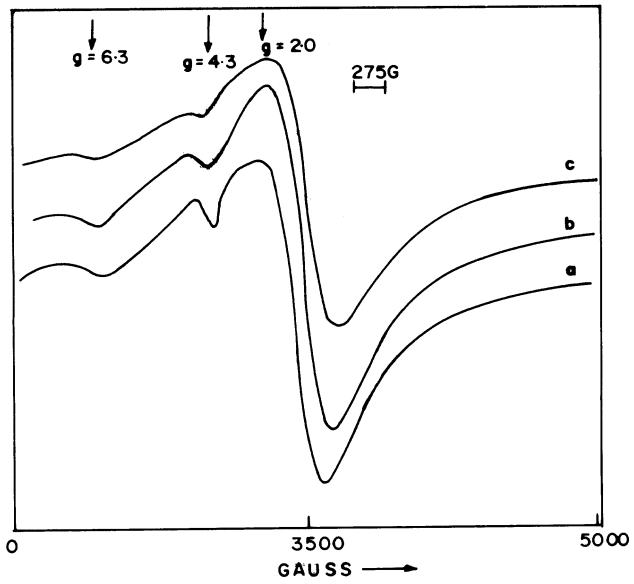

Figure 3. ESR spectra for Fe-FER samples: (a) as-synthesized Fe-FER-IIb and (b) calcined Fe-FER-IIb and (c) as-synthesized Fe-FER-Ic.

the Mössbauer spectra complements an expulsion of (about one third of the original tetrahedral coordination) Fe^{3+} upon calcination. Further detailed Mössbauer studies under different environments are under investigation.

The ESR spectra of as-synthesized (Fe-FER-IIb (figure 3a) and Fe-FER-Ic (figure 3c), table 1) and calcined samples (Fe-FERIIb cal (figure 3b); table 1) exhibit three signals corresponding to g values of ~ 2.0, 4.3 and 6.3. On the basis of signal assignment [28–43], the signal with g value ~ 2.0 can be assigned to Fe^{3+} in cationic site location, while the signal corresponding to a g value of 4.3 may be due to isomorphously substituted Fe^{3+} in the zeolite framework. In contrast, a signal at $g = 2.0$ was observed for $FePO_4$ where Fe^{3+} has tetrahedral co-ordination [42]. Lin et al. [44] suggested that in the case of $FePO_4$ there is no charge disymmetry while in the case of zeolites a charge disymmetry exists and hence the signal with $g = 4.3$ may be assigned to Fe^{3+} in a distorted tetrahedral environment. Furthermore, Goldfarb et al. [45] observed a single signal in the ESR spectra of Fe-SOD suggesting that on the basis of ESR data alone it is very difficult to assign the sites occupied by Fe in the framework. The ESR signal with g value = 6.3 may be due to the presence of Fe^{3+} complexes or due to distortion of symmetry [43]. Upon calcination the signal corresponding to $g = 4.3$ reduces in intensity indicating one third loss of Fe^{3+} from the framework (figure 3b, sample Fe-FER-IIb cal). This observation is complementary to the data obtained from Mössbauer spectroscopy.

The diffuse reflectance spectra of the as-synthesized Al-FER, Fe-FER-Ib and Fe-FER-IIc samples (figure 4, curves a, b and c respectively) showed three low intensity peaks around 363, 388, and 417 nm. Goldfarb et al. [45] also observed low intensity peaks in the same region for Fe-SOD, Fe-LTL2, Fe-MAZ-2 and Fe-FAU. Lin et al. [44] assigned these to weak "forbidden" d–d transitions and from the CFSE (crystal field stabilizing energy) values obtained, they concluded that Fe^{3+} has a tetrahedral environment. Furthermore, the as-synthesized as

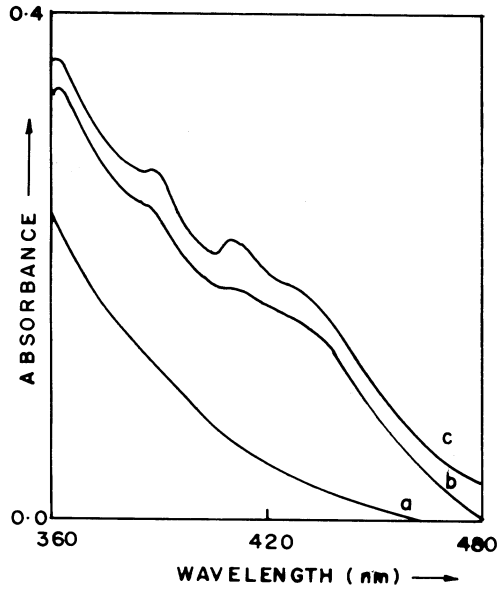

Figure 4. Diffuse reflectance spectra of as-synthesized (a) Al-FER; (b) Fe-FER-Ib and (c) Fe-FER-IIc samples.

well as the calcined samples did not show a broad shoulder (around 630 nm) in the UV spectra indicating the absence of Fe_2O_3 clusters.

The IR spectra of Fe-FER-IIb, Fe-FER-Ib and Al-FER with $SiO_2/Fe_2O_3 = 60$ are presented in figure 5 curves a, b and c. The strong absorption band in 1000–1200 cm^{-1} region is assigned to internal vibration of SiO_4, AlO_4/FeO_4 tetrahedra, which are also reported for silica and quartz [46]. The absorbance at 580 cm^{-1} was assigned by Jacobs et al. [47] to a highly distorted double five-membered ring present in the zeolite framework structure. An additional band around 650 cm^{-1} was observed in the case of Fe-FER; this band has been assigned to Si–O–Fe linkages by Szostak et al. [25]. The strongest band around 1090 cm^{-1} is related to the asymmetric stretching vibrations of T–O linkage. This band is shifted to a lower frequency for ferrisilicate (Fe-FER) samples as compared to Al-FER. The shift in frequency is consistent with the observation made by Szostak et al. [25] and can be explained on the basis of T–O bond distance. Flaningen and Grose [48] have established evidence for phosphorus substitution in the zeolite framework by using an IR technique. Substitution of phosphorus in the framework showed the shift in the main asymmetric bands towards higher frequency. Similarly, the substitution of Fe^{3+}, in the zeolite framework should show some change. However, due to the longer Fe–O bond distance (1.97 Å) the band which occurs at ~ 1100 cm^{-1} shifts towards lower frequency.

The representative thermoanalytical curves of zeolite Al-FER, Fe-FER-Ic and Fe-FER-IId samples in their as-synthesized form are illustrated in figure 6. The TG curves indicate continued weight loss ($\sim 2.0\%$) mainly due to the dehydration occurring from ferrierite cavity in the low temperature range 575 K. The DTA curves reveal an endothermic effect with a minimum at 370 K and a strong exothermic effect at around 770 K, indicating a major transformation. This positive heat effect is attributed to the oxidative decomposition of the organic moieties occluded in the zeolite framework. Further, there is no major transformation observed in the temperature range 775 to 1200 K confirming the thermal stability of the Fe-FER structure.

The scanning electron micrographs for Fe-FER-Ib and Fe-FER-IIb (ref. table 1) are illustrated in figures 7a and 7b respectively. In the case of Fe-FER-Ib (with added aluminum, figure 7a) an assembly of small aggregates having average particle size of around 3 μm was observed. This can be due to longer nucleation periods which in turn gives a large number of agglomerates resulting into average 3 μm particles. While the Fe-FER-IIb (with seeds) sample (figure 7b) comprises of uniform small crystallites having size around 1–2 μm. This may be due to the presence of seed precursors which initiate early nucleation and give rise to uniform particle growth.

The sorption capacities observed for the Na/Fe-

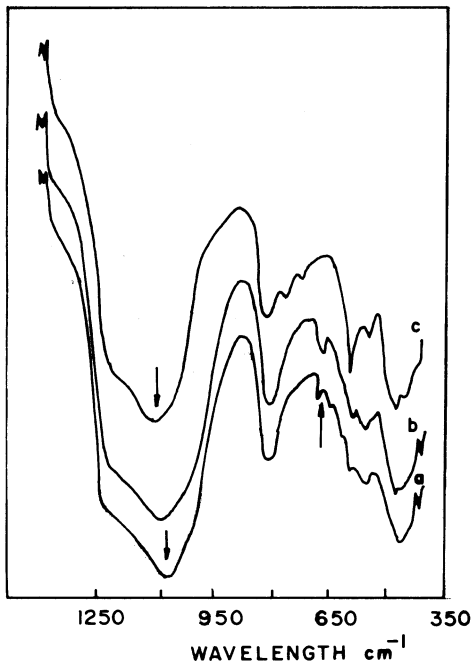

Figure 5. Framework infrared spectra of: (a) Fe-FER-IIb; (b) Fe-FER-Ib and (c) Al-FER samples.

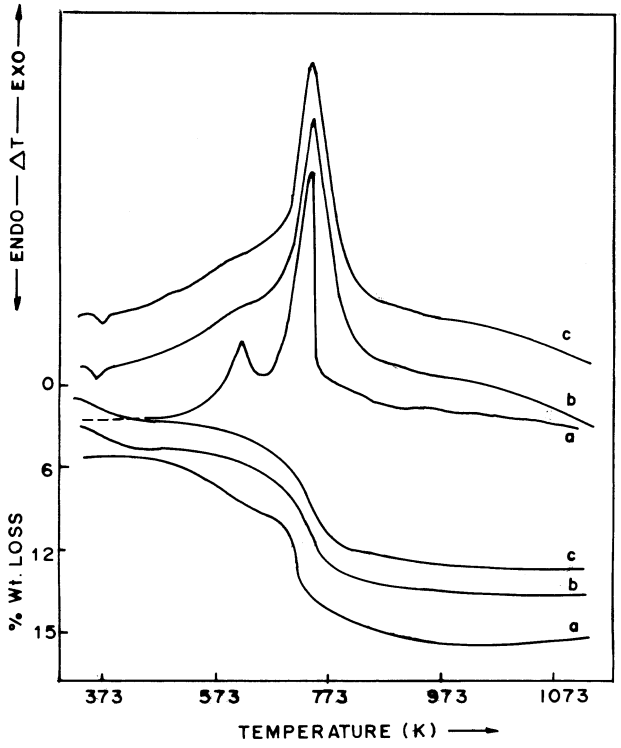

Figure 6. Thermoanalytical curves for (a) Al-FER; (b) Fe-FER-Ic and (c) Fe-FERIId samples.

a

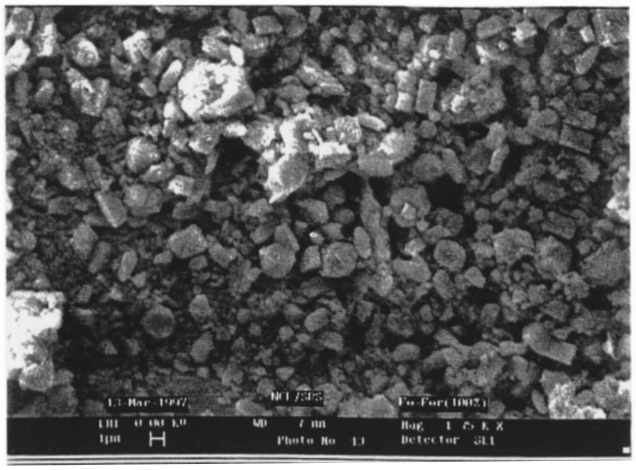

b

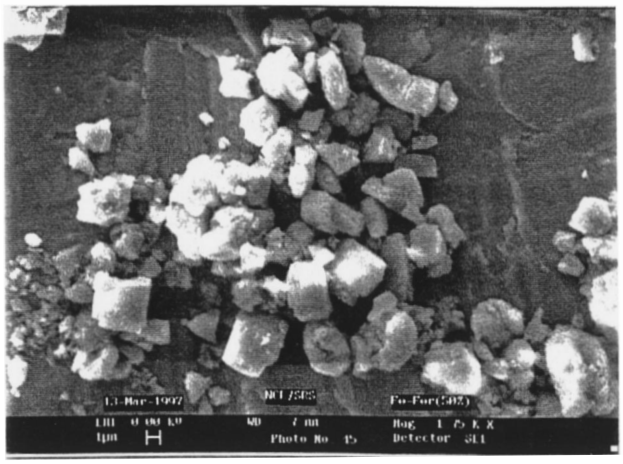

Figure 7. Scanning electron micrographs for (a) Fe-FER-Ib and (b) Fe-FER-IIb samples.

FER series are listed in table 3. The sorption values for *n*-hexane are found to be almost constant. Considering the kinetic diameter of *n*-hexane to be 3.1 Å, its sorption behavior suggests complete pore filling with end to end configuration. However, water sorption decreases with increase in SiO_2/Fe_2O_3 ratio. The water sorption gives the extent of hydrophobicity with varying SiO_2/Fe_2O_3 ratio. The low cyclohexane sorption capacity for all the samples suggests that although the pore entry for FER type zeolite is characterized by 10 T-ring apertures, its elliptical nature (5.5×4.3 Å) seems to make it inaccessible to cyclohexane molecules.

6. Catalytic properties

The Fe-FER samples were found to be active for *n*-hexane oxidation using H_2O_2 (48 wt%). The results for the reaction are summarized in table 4, the selectivity for hexane-3-one was found to be higher. It was observed that Al-FER as well as samples belonging to Fe-FER-I series did not exhibit any catalytic activity. This can be attributed to the presence of Fe–Al mixed oxides in the Fe-FER-I system. Ratnasamy and Kumar [49] have also remarked that the presence of Al in ferrisilicates inhibits their catalytic activity. A blank reaction to investigate the leaching effect of Fe^{3+} was carried out and it was estimated that 0.015% of Fe had leached out during the reaction. Based on this blank reaction results it is believed that a small quantity of leached iron is unlikely to shift the reaction equilibrium. Further investigations on catalytic reactions are in progress at NCL.

Table 3
Sorption properties of Fe-FER series

Sample	Product SiO_2/M_2O_3	Product SiO_2/Fe_2O_3	Amount adsorbed g/100 g of Fe-FER zeolite		
			H_2O	*n*-C_6H_{14}	C_6H_{12}
Fe-FER-Ib	34	63	10.5	13.0	2.0
Fe-FER-IIa	–	25	12.5	13.5	2.5
Fe-FER-IIb	–	34	12.0	13.2	2.2
Fe-FER-IId	–	73	7.4	12.9	1.0
Al-FER	32	–	10.0	13.0	2.2

7. Conclusions

The synthesis of ferrisilicate analogs of FER type zeolite using pyrrolidine as template and FER seeds precursor has been demonstrated. Isomorphous substitution of Fe^{3+} for Al^{3+} has been further supported by ^{57}Fe Mössbauer spectroscopy which typically shows a broad singlet at 0.25 mm s^{-1} and ESR data exhibit a signal corresponding to $g = 4.3$ for as-synthesized Fe-FER. Upon calcination the Fe-FER developed a slight buff color which is indicative of loss of about one third of Fe^{3+} from the framework. Fe-FER samples are found to be active in *n*-hexane oxidation reactions.

Table 4
n-hexane oxidation on Fe-FER [a]

Sample	% conv.	Product selectivity			
		1-al	2-ol	3-one	3-ol
Fe-FER-Ia	–	–	–	–	–
Fe-FER-Ib	4.0	0.02	4.35	6.32	5.93
Fe-FER-IIb	15	6.4	14.56	22.32	11.6
Fe-impregnated	2.5	0.02	4.00	6.70	4.04
Al-FER	–	–	–	–	–

[a] Reactant moles: *n*-hexane : H_2O_2 : acetonitrile = 1 : 1 : 7.5; catalyst 20%. Temperature 353 K, time 20 h.

Acknowledgement

RKA thanks C.S.I.R. for a senior research fellowship.

References

[1] H.W. Kovenhoven and W.H.J. Stork, US Patent 3,208,395.
[2] P. Ratnasamy, R.B. Borade, S. Sivasankar, V.P. Shiralkar and S.G. Hegde, *Proc. Int. Symp. on Zeolites Catalysts*, Siofok 1985, p. 137.
[3] W.J. Ball, Stud. Surf. Sci. Catal. 28 (1986) 137.
[4] R. Szostak and T.L. Thomas, J. Catal. 100 (1986) 555.
[5] A.N. Kotasthane, V.P. Shiralkar, S.G. Hegde and S.B. Kulkarni, Zeolites 6 (1986) 253.
[6] G.C. Alis, P. Frenken, A. de Boer, A. Swolfs and M.A. Hefni, Zeolites 7 (1987) 319.
[7] R.B. Borade, Zeolites 7 (1987) 398.
[8] B. Wichterlova, S. Beran, S. Bednarova, K. Nedomova, L. Dudinova and P. Jiru, in: *Innovation in Zeolite Materials Science*, Stud. Surf. Sci. Catal., Vol. 37, eds. P.J. Grobet et al., (Elsevier, Amsterdam, 1987) p. 199.
[9] G. Doppler, R. Lehnert, L. Marosi and A.X. Trautwein, in: *Innovation in Zeolite Materials Science*, Stud. Surf. Sci. Catal., Vol. 37, eds. P.J. Grobet et al. (Elsevier, Amsterdam, 1987) p. 215.
[10] R. Kumar and P. Ratnasamy, J. Catal. 121 (1990) 89.
[11] R. Szostak and T.L. Thomas, J. Chem. Soc. Chem. Commun. (1986) 113.
[12] (a) R. Kumar, A. Thangaraj, R.N. Bhat and P. Ratnasamy, Zeolites 10 (1990) 85;
(b) C.N. Flaningen, B.M.T.K. Lok, R.L. Palton and S.T. Wilson, Stud. Surf. Sci. Catal. 28 (1986) 109.
[13] P. Ratnasamy, A.N. Kotasthane, V.P. Shiralkar, A. Thangaraj and S. Ganapathy, in: *Advances in Zeolite Synthesis*, ACS Sympos. Ser., ed. M. Ocelli (Am. Chem. Soc., Washington, 1989) p. 405.
[14] H.H. Mooiweer, K.P. de Jong, B. Kraushaar-Czarnetzki, W.H.J. Stork and B.C.H. Krutzen, Stud. Sci. Surf. Catal. 84 (1994) 2327.
[15] C.L. O'Young, R.J. Pellet, D.G. Casey, J.R. Ugolini and R.A. Sawicki, J. Catal. 131 (1995) 467.
[16] C.T.W. Chu and C.D. Chang, J. Phys. Chem. 89 (1985) 1569.
[17] C.J. Plank, E.J. Rosinski and M.K. Rubin, US Patent 4016 245 (1977).
[18] R.B. Borade and A. Clearfield, Zeolites 14 (1994) 458.
[19] W. Xu, J.X. Dond, J. Li, J. Ma and T. Dou, Zeolites 12 (1988) 299.
[20] D. Seddon and T.V. Whittam, Eur. Patent B-55 529 (1985).
[21] T.V. Whittam, Eur. Patent A 103 981 (1984).
[22] B. Sulikowsler and J. Klinnowski, J. Chem. Soc. Chem. Commun. (1989) 1289.
[23] V. Satoru, T. Minchiro and K. Mitsue, Clay Sci. 7 (1988) 185.
[24] R.B. Borade and A. Clearfield, J. Chem. Soc. Chem. Commun. 19 (1996) 2267.
[25] R. Szostak, V. Nair and T.L. Thomas, J. Chem. Soc. Faraday Trans. I 83 (1987) 487.
[26] A. Meagher, V. Nair and R. Szostak, Zeolites 8 (1988) 3.
[27] R.L. Garten, W.N. Delgass and M.J. Boudart, J. Catal. 18 (1970) 90.
[28] G. Zi, T. Dake and Z. Ruiming, Zeolites 8 (1988) 453.
[29] T. Inui, H. Nagata, T. Takeguchi, S. Iwamoto, H. Matsuda and M. Inoue, J. Catal. 6 (1993) 328.
[30] P. Ratnasamy and R. Kumar, Catal. Today 9 (1991) 328.
[31] B. Wichterlova, Zeolites 1 (1981) 181.
[32] J. Novalkova, L. Kubelkova, B. Wichterlova, T. Thomas and Z. Dolejsek, Zeolites 2 (1982) 217.
[33] B. Wichterlova, J. Novakova, L. Kukelhova and P. Milkusik, Zeolites 5 (1985) 21.
[34] A.E. Ojo, J. Dwyer and R.V. Parish, in: *Zeolites: Facts, Figures, Future*, eds. P.A. Jacobs and R.A. van Santen (Elsevier, Amsterdam, 1989) p. 227.
[35] P. Wenqin, Q. Shilun, K. Qiubin, W. Zhiyun and P. Shaoji, in: *Zeolites: Facts, Figures, Future*, eds. P.A. Jacobs and R.A. van Santen (Elsevier, Amsterdam, 1989) p. 281.
[36] P.N. Joshi, S.V. Awate and V.P. Shiralkar, J. Phys. Chem. 97 (1993) 9749.
[37] B.D. McNicol and G.T. Pott, J. Catal. 25 (1972) 223.
[38] L.M. Kustov, V.B. Kazansky and P. Ratnasamy, Zeolites 7 (1987) 79.
[39] E.G. Derouane, M. Mestdagh and L. Vielvoye, J. Catal. 33 (1974) 90.
[40] L.E. Iton, R.B. Beal and D.T. Hodul, J. Chem. Phys. 21 (1983) 151.
[41] J. Patarin, Doctrat et Science Thesis, Mulhouse, France (1988).
[42] Nat. Bur. Stand. (USA) Monogr. 25, sec 15 1978.
[43] T. Castner Jr., G.S. Newell, W.C. Holton, G.A. Silchter, J.E. Crowford and G.A. Nelson, Collides Surf. 4 (1982) 331.
[44] D.H. Lin, G. Coudurier and J.C. Vedrine, in: *Zeolites: Facts, Figures, Future*, eds. P.A. Jacobs and R.A. van Santen (Elsevier, Amsterdam, 1989) p. 1431.
[45] D. Goldfarb, M. Bernado, K.G. Strohmaier, D.E.W. Vaughan and H. Thomann, J. Am. Chem. Soc. 116 (1994) 6344.
[46] M. Ghamami and L.B. Sand, Zeolites 2 (1982) 143.
[47] P.A. Jacobs, H.K. Bayer and J. Valyon, Zeolites 1 (1981) 161.
[48] E.M. Flaningen and R.W. Grose, Adv. Chem. Ser. 101 (1971) 76.
[49] P. Ratnasamy and R. Kumar, Catal. Today 9 (1991) 329.